LUND UNIVERSITY

The Faint Optical Stellar Luminosity Function in the Ursa Minor Dwarf Spheroidal Galaxy

Feltzing, Sofia; Gilmore, G; Wyse, R F G

Published in:
Astrophysical Journal

DOI:
10.1086/311988

1999

Link to publication

Citation for published version (APA):
Feltzing, S., Gilmore, G., & Wyse, R. F. G. (1999). The Faint Optical Stellar Luminosity Function in the Ursa Minor Dwarf Spheroidal Galaxy. *Astrophysical Journal*, *516*(1), L17-L20. https://doi.org/10.1086/311988

Total number of authors:
3

General rights
Unless other specific re-use rights are stated the following general rights apply:
Copyright and moral rights for the publications made accessible in the public portal are retained by the authors and/or other copyright owners and it is a condition of accessing publications that users recognise and abide by the legal requirements associated with these rights.
• Users may download and print one copy of any publication from the public portal for the purpose of private study or research.
• You may not further distribute the material or use it for any profit-making activity or commercial gain
• You may freely distribute the URL identifying the publication in the public portal

Read more about Creative commons licenses: https://creativecommons.org/licenses/

Take down policy
If you believe that this document breaches copyright please contact us providing details, and we will remove access to the work immediately and investigate your claim.

LUND UNIVERSITY

PO Box 117
221 00 Lund
+46 46-222 00 00

THE ASTROPHYSICAL JOURNAL, 516:L17–L20, 1999 May 1
© 1999. The American Astronomical Society. All rights reserved. Printed in U.S.A.

THE FAINT OPTICAL STELLAR LUMINOSITY FUNCTION IN THE URSA MINOR DWARF SPHEROIDAL GALAXY[1]

SOFIA FELTZING[2,3]
Royal Greenwich Observatory, Madingley Road, Cambridge CB3 0EZ, UK
GERARD GILMORE
Institute of Astronomy, Madingley Road, Cambridge CB3 0HA, UK
AND
ROSEMARY F. G. WYSE
Johns Hopkins University, Department of Physics and Astronomy, Baltimore, MD 21218
Received 1998 December 28; accepted 1999 February 22; published 1999 March 9

ABSTRACT

Analyses of their internal stellar kinematics imply that the dwarf spheroidal (dSph) companion galaxies to the Milky Way are among the most dark matter–dominated systems known. Should there be significant dark matter in the form of faint stars in these systems, the stellar luminosity function must be very different from that of a similar metallicity globular cluster, for which there is no evidence for dark matter. We present the faint stellar luminosity function in the Ursa Minor dSph, down to a luminosity corresponding to ∼0.45 $M_\odot$, derived from new deep *Hubble Space Telescope*/WFPC2 data. We find a remarkable similarity between this luminosity function, and inferred initial mass function, and those of the globular cluster M92, a cluster of similar age and metallicity to the Ursa Minor dSph.

Subject headings: dark matter — galaxies: individual (Ursa Minor) — galaxies: kinematics and dynamics — galaxies: stellar content — stars: luminosity function, mass function

1. INTRODUCTION

Most of the dwarf spheroidal (dSph) companions of the Milky Way have stellar velocity dispersions that are in excess of those expected if stars with a normal mass function dominate their internal gravitational potentials (see Mateo 1998 for a recent review). Neither orbital motions within stellar binaries (Hargreaves, Gilmore, & Annan 1996; Olszewski, Pryor, & Armandroff 1996) nor Galactic tidal effects (e.g., Piatek & Pryor 1995) can inflate the internal velocity dispersions enough to explain these measurements. Rather, the stellar kinematics imply the presence of gravitationally dominant dark matter, concentrated on small length scales, with a mass-to-light ratio of a factor of 10–50 above those of normal stellar populations. Could the dark matter be low-mass stars? Stars of mass less than ∼0.5 $M_\odot$ have *V*-band mass-to-light ratios above 10 (in solar units) and are thus viable candidates, provided that the stellar initial mass function (IMF) in these systems is very different from that of the solar neighborhood or that in globular clusters.

A direct test of this hypothesis is provided by comparison of the faint stellar luminosity function in a dSph galaxy with that of a stellar system of similar age and metallicity but which is known not to contain dark matter. Empirical comparison between the luminosity functions minimizes the uncertainties in the transformation between mass and light (see D'Antona 1998 for a recent discussion of this point). In addition to its possible relevance to dark matter problems, the IMF of low-mass stars in a wide variety of astrophysical systems is of considerable intrinsic interest (see, e.g., papers in Gilmore & Howell 1998). Various indirect means to determine the low-mass stellar IMF in external galaxies have been applied, particularly analyses of optical and infrared surface brightnesses (Carr 1994). The results are either inconclusive or apply only to the very outer regions of galaxies (e.g., Davis, Feigelson, & Latham 1980; Gilmore & Unavane 1998). Only direct star counts can provide unambiguous results.

We here derive the faint stellar luminosity function in the Ursa Minor dwarf spheroidal galaxy (distance modulus 19.11 ± 0.1, or 66 ± 3 kpc; Mateo 1998). The internal stellar velocity dispersion of ∼10 km s^{-1} (Hargreaves et al. 1994; Olszewski, Aaronson, & Hill 1995) implies a total mass-to-light ratio of $(M/L)_V \sim 80$ (summarized in Mateo 1998). This large mass-to-light ratio contrasts with the typical value of $(M/L)_V$ for globular clusters of ∼2 (e.g., Djorgovski & Meylan 1994; Merritt, Meylan, & Mayor 1997). Ground-based photometry of the red giant branch and main-sequence turnoff in the UMi dSph are consistent with essentially a monoage (∼15 Gyr) and monometallicity ([Fe/H] ∼ −2.2) stellar population (Olszewski & Aaronson 1985) similar to that of the old metal-poor halo globular clusters, in particular to M92. These narrow ranges of age and metallicity contrast with most of the other dSph companion galaxies in which there have been complex star formation histories and chemical evolution (e.g., Mateo 1998; Hernandez, Gilmore, & Valls-Gabaud 1999). The only other derivation of a luminosity function for a dSph is that by Grillmair et al. (1998) for the upper main sequence of the Draco dSph galaxy; in that case, the analysis is complicated by the significant metallicity spread in this galaxy (e.g., Shetrone, Bolte, & Stetson 1998). Our analysis of the stellar luminosity function in the Ursa Minor dSph is greatly simplified by the lack of a significant spread in either age or metallicity, since this lack implies a unique relationship between stellar luminosity and mass. In this analysis we compare directly our *Hubble Space Telescope* (*HST*) luminosity function for UMi with the luminosity function derived for M92 by Piotto, Cool, & King (1997).

[1] Based on observations with the NASA/ESA *Hubble Space Telescope*, obtained at the Space Telescope Science Institute, operated by the Association of Universities Inc., under NASA contract NAS5-26555.
[2] Also at Institute of Astronomy, Madingley Road, Cambridge CB3 0HA, UK.
[3] Present address: Lund Observatory, Box 43, 221 00 Lund, Sweden.

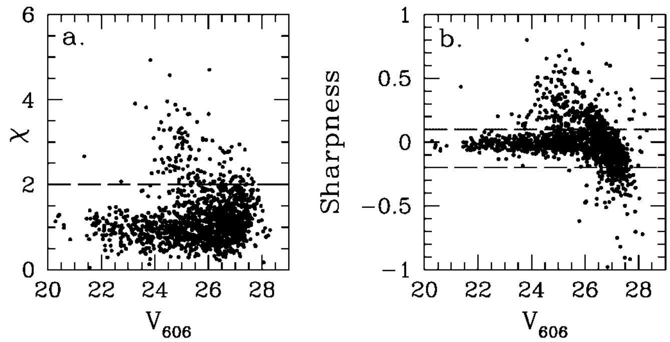

FIG. 1.—Statistical parameters χ and sharpness for WF2, F606W for the UMi data set, vs. V_{606} magnitude. The applied cuts are shown as dashed lines.

2. DEEP *HST* STAR COUNTS IN THE URSA MINOR DWARF SPHEROIDAL GALAXY

We obtained deep imaging data with the *Hubble Space Telescope*, using all of WFPC2, STIS, and NICMOS in a field close to the center of the Ursa Minor dSph (program GO-7419, Principal Investigator R. F. G. Wyse). The correction of the data in this field for contamination by foreground stars and background galaxies required acquisition of similarly exposed data for a field at ~2 tidal radii away from the Ursa Minor dSph, but at similar Galactic coordinates to the main UMi field ($\ell = 105°$, $b = 45°$). The STIS and NICMOS data will be discussed elsewhere; here we present the faint optical stellar luminosity function derived from our WFPC2 data.

2.1. *Observations and Data Reduction*

The WFPC2 fields in the Ursa Minor dSph (UMi) and offset from the galaxy (UMi-off) have WFALL coordinates of (α_{2000}, δ_{2000}) = ($15^h08^m00^s$, +67°09′01″) and ($14^h55^m35^s$, +68°36′00″), respectively. Each field was exposed for 8 × 1200 s in each of the F606W and F814W filters. Standard *HST* data reduction techniques were followed, using the IRAF[4] STSDAS routines. Photometry on the reduced images used DAOPHOT, with the recipe detailed by Cool & King (1995), and TinyTim point-spread functions, with calibration following Holtzman et al. (1995a, 1995b). The scatter in the zero points and photometric calibrations is ~6%, providing a calibration uncertainty that is small compared to the 0.5 mag binning we adopt below. Identical procedures were applied to both the UMi and the offset data sets.

The main feature of note in the present data reduction concerns the completeness and reliability of faint source detection. Since we wish to go as faint as possible while retaining reliability, we deliberately adopt a low value of the detection threshold and subsequently use two-color data to remove the inevitably large number of spurious detections. The appropriate detection threshold was identified by running DAOFIND using different values and examining the number of detections as a function of $n \times \sigma_{\rm bkgrnd}$. We adopted a threshold of 2.5 $\sigma_{\rm bkgrnd}$, which provided 4000–5000 detections on each WF chip. Two statistics on the goodness of fit—χ and sharpness—are used to determine which detections should be kept as bona fide stars and which should be rejected. The sharpness parameter aids in the separation between stars and resolved objects, such as background galaxies. An example of the ranges of the values of these parameters for the WF2 image of the UMi field is shown in Figure 1, in which the threshold values we adopted are indicated. Again, the same parameter values were adopted for the images of the offset field. Finally, the stellar coordinates from the independently reduced F606W and F814W images were cross-identified, using a matching radius of 1 pixel, to provide a list of all stellar objects detected and measured in both *V* and *I* bands.

[4] IRAF is distributed by National Optical Astronomy Observatories, operated by the Association of Universities for Research in Astronomy, Inc., under contract with the National Science Foundation.

TABLE 1

V-BAND STELLAR LUMINOSITY FUNCTION DERIVED FROM THE CMD

	COUNTS			COMPLETENESS				
$V_{\rm F606W}$	WF2	WF3	WF4	WF2	WF3	WF4	UMI-OFF	FINAL LF
23.25	24	30	17	1.00	1.00	1.00	1	70
23.75	40	32	27	1.00	1.00	1.00	1	98
24.25	42	46	37	0.96	0.96	0.97	3	126
24.75	52	60	45	0.94	0.93	0.97	6	160
25.25	74	58	56	0.94	0.94	0.95	2	197
25.75	56	63	43	0.91	0.90	0.91	3	175
26.25	57	77	65	0.85	0.81	0.86	1	237
26.75	45	59	57	0.71	0.68	0.77	3	220
27.25	73	58	44	0.50	0.51	0.50	2	344
27.75	9	34	25	0.28	0.30	0.33	3	211

2.2. *Completeness Corrections*

The completeness of the data was determined by adding artificial stars to the original images and then reprocessing them as described above; the fraction of the artificial stars that is recovered provides the estimate of the completeness. The number of artificial stars added must be sufficiently high to provide reasonable statistical accuracy, but not so high as to change the level of crowding in the image. In each WF chip we detect in total about 450 stellar objects, so the optimum number of artificial stars should be a few hundred for a given magnitude. We experimented with adding the stars either in a grid pattern, with small random increments in *x* and *y* to avoid sitting exactly at pixel centers, or completely randomly; full details are described in Feltzing & Gilmore (1999, in which we also discuss tests based on various subsets of the total integrations).

Briefly, 266 stars, all with the same magnitude, were added to the F606W image of each WF chip. Each artificial star provides an independent test. The resulting images were analyzed as described above, giving the completeness for that particular magnitude. This process was repeated in 0.5 mag steps to the limiting magnitude of the data. The completeness function for the *I*-band data was obtained through the same procedure, but with the magnitudes for F814W chosen so that the mean ridge line of the color-magnitude diagram (CMD) was reproduced. The completeness function for CMD-based luminosity functions was obtained by the further requirement that the recovered star should be detected in both *V* and *I*. The resulting completeness function for the CMD-derived *V*-band luminosity function (LF) is given in Table 1. The estimated completeness functions for the three WF chips agree extremely well, as detailed in Table 1, reflecting the statistical robustness of our technique. The completeness function, based on the CMD, for the *I*-band LF is just that for the *V* band, but with the corresponding magnitude being offset by the mean color of Figure 2*a*. The 50% completeness of the *V*-band luminosity function derived on the basis of the CMD data is 27.25 mag, while that for the *I* band is 50% at 26.25 mag.

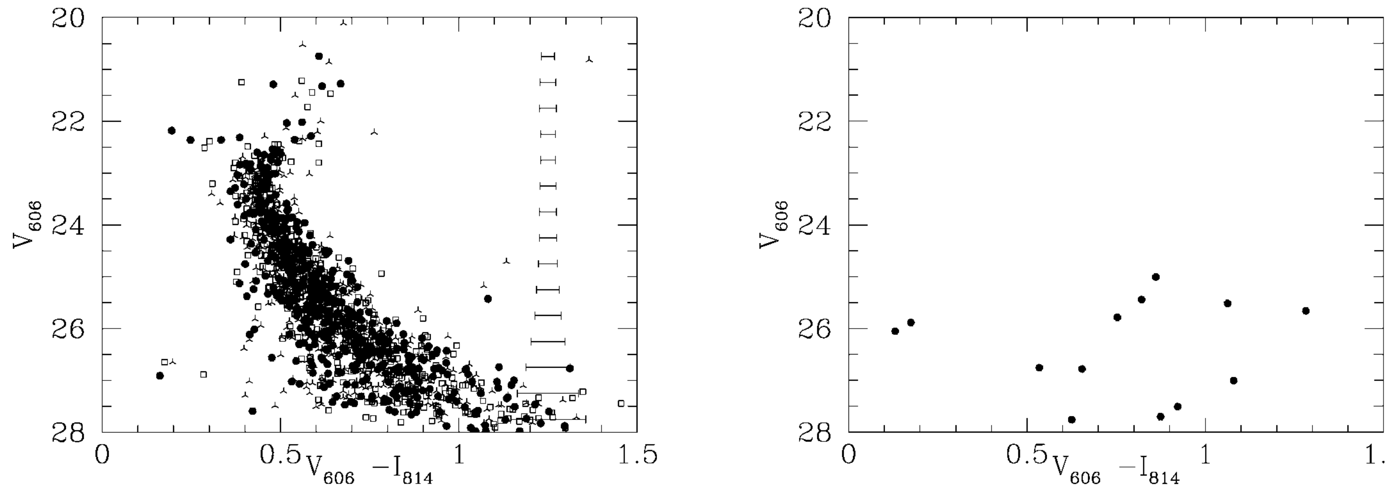

FIG. 2*a*

FIG. 2*b*

FIG. 2.—*HST* inflight color-magnitude diagram for (*a*) the UMi field and (*b*) the offset field. The different symbols in panel *a* denote different WF chips. The 1 σ photometric uncertainties in color are as indicated; those in the magnitude are approximately a factor of 1.4 smaller and are not shown for clarity.

3. THE COLOR-MAGNITUDE DIAGRAMS

Prior to comparison of the M92 and UMi luminosity functions, we first confirm, by inspection of our derived CMD for UMi, that they both have similar stellar populations and that our data appear reliable. We consider briefly the width of the main sequence, the presence of "blue stragglers," and the stars detected in the offset field.

The color-magnitude diagrams for the UMi and the UMi-off data sets are shown in Figures 2*a* and 2*b*, with 1 σ photometric uncertainties as indicated. Note that the ridge line of M92 follows that of our UMi data (not shown for clarity). The apparent width of the main sequence in the UMi dSph is dominated by photometric scatter. Any metallicity dispersion or line-of-sight depth is undetected. Unresolved binaries might affect the derived luminosity function comparison, if the binary fraction or the binary primary-secondary mass function were very different in the UMi dSph compared to that of M92. We detect a marginally significant redward asymmetry of 0.02 mag in the UMi color distribution, consistent with a small binary fraction. For the relevant mass range, the slope of the apparent luminosity function is not sensitive to variations in binarism of this order (Kroupa, Tout, & Gilmore 1991; their Fig. 3), especially given the large bins in apparent magnitude used below. The CMD of the UMi field contains a small number (~5) of stars blueward of the main-sequence turnoff, consistent with the frequency of blue stragglers derived by Olszewski & Aaronson (1985). The CMD of the offset field contains no such stars, strengthening their identification with the Ursa Minor dSph. Interestingly, these stars are too blue to fit a younger isochrone with the same metallicity as the dominant population of UMi. Their nature remains uncertain (more metal poor?). These few stars are at brighter magnitudes than is relevant for our luminosity function comparison.

The most obvious consequence of Figure 2 is that the UMi-off CMD contains so few stars that contamination of the UMi CMD and luminosity function by foreground stars or by background unresolved galaxies is not a concern. The star counts in the offset field are also presented in Table 1, in the column UMi-off. Our luminosity function in the *V* band derived from the CMD is given in Table 1. Note that we have confirmed that these results are insensitive to the choice of bin center.

4. ANALYSIS AND DISCUSSION

Care is needed in the choice of globular cluster data, since internal dynamical relaxation effects and external tidal limitation modify the observed faint luminosity (and mass) function from the initial one. Mass segregation within a globular cluster depends on many unknown parameters, including the initial binary fraction and the initial core density. Piotto et al. (1997) have determined the faint stellar luminosity function for M92 in a field at ~5 times the cluster's half-light radius. Happily, a comparison of the luminosity functions derived from two fields at 3.5 and 5 half-mass radii within M92 shows that any significant mass segregation is restricted to magnitudes fainter than those of our comparison here (Andreuzzi et al. 1998). Modifications to the global LFs by external tidal effects such as disk shocking are observed in many Galactic globular clusters. Elson et al. (1999) show that the stellar mass function of M92 is essentially unmodified by external dynamical effects. The Piotto et al. (1997) LF is therefore a fair measure of the IMF in M92. Their observations are in the same *HST* passbands as our UMi data and are reduced and calibrated in the same way as adopted here.

A straightforward comparison of the faint (unevolved stars) luminosity functions in *V* and in *I* of the Ursa Minor dSph with those for M92 thus provides a direct comparison of the stellar IMFs in the range of interest here. This is shown in Figure 3, which contains the main result of this Letter: the remarkable agreement between the faint stellar luminosity function of a system in which there is no inferred dark matter and a system in which very significant amounts of dark matter are inferred. Further, these two systems—a globular cluster and a dSph galaxy—are at opposite extremes of stellar number density, with the central *V*-band surface brightness of M92 being 15.6 mag arcsec^{-2} (Harris 1996), while that of the UMi dSph is 25.5 mag arcsec^{-2} (Mateo 1998).

The mass corresponding to our 50% completeness limit may be estimated from stellar models. The models of Baraffe et al. (1997) for low-mass stars of metallicity -2 dex, transformed to the appropriate *HST* filters (their Fig. 5) and at the distance and reddening [$E(V-I) = 0.045$] of UMi, translate these completeness levels to masses of ~0.45 $M_\odot$. The VandenBerg isochrones for [Fe/H] = -2.2 dex, transformed into the *HST*

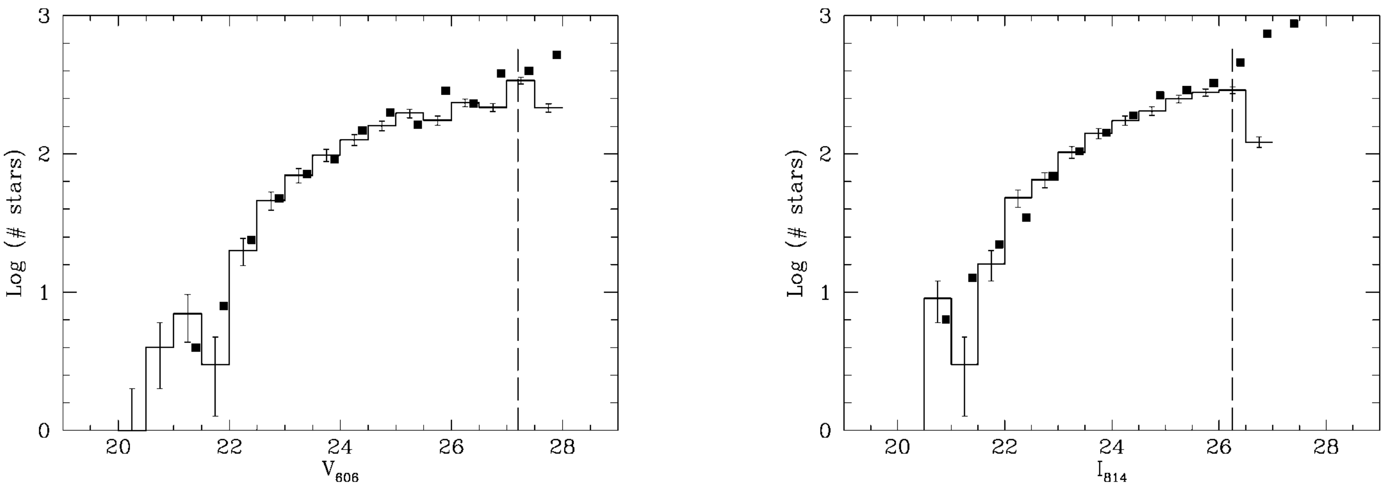

FIG. 3.—Comparison between the UMi completeness-corrected luminosity functions derived from the CMD with that of the globular cluster M92 (*filled squares*); the *V* band (*left*) and the *I* band (*right*). The vertical dashed lines indicate the 50% completeness limits. The normalizations of the *V* and *I* band were applied using the CMD colors, providing a consistency check on the data.

filters by G. Worthey (1998, private communication), provide consistent results. Should one wish to adopt a mass-luminosity relation, then the resulting stellar mass function for the UMi dSph would be essentially that derived by Piotto et al. (1997) for M92.

The observations presented here demonstrate that the faint stellar luminosity function in the Ursa Minor dSph, measured down to a luminosity corresponding to ∼0.45 $M_{\odot}$, is indistinguishable from that of the globular cluster M92. This precludes stars in this mass range from being any part of the explanation of the high velocity dispersions observed, and implied high dark matter content, in the UMi dSph galaxy. Furthermore, the similarity of the stellar luminosity and mass functions of the UMi dSph and of M92 over the whole range observed to date provides no evidence for any difference in low-mass IMFs as a function of environment, for low-metallicity stars.

Support for this work was provided by NASA through grant GO-7419 from the Space Telescope Science Institute, which is operated by the Association of Universities for Research in Astronomy Inc., under NASA contract NAS5-26555. S. F. acknowledges financial support from the Swedish Natural Research Council under their postdoctoral fellowship program. We thank Jay Gallagher, Rachel Johnson, Tammy Smecker-Hane, and Nial Tanvir for comments and discussions and are grateful to Giampaolo Piotto for making the M92 data available to us.

REFERENCES

Andreuzzi, G., Buonanno, R., Iannicola, G., & Marconi, G. 1998, Mem. Soc. Aston. Italiana, 69, 263
Baraffe, I., Chabrier, G., Allard, F., & Hauschildt, P. 1997, A&A, 327, 1054
Carr, B. 1994, ARA&A, 32, 531
Cool, A. M., & King, I. R. 1995, *HST* Postcalibration Workshop, ed. A. Koratkar & C. Leitherer (Baltimore: STScI), 290
D'Antona, F. 1998, in ASP Conf. Ser. 142, The Stellar Initial Mass Function, ed. G. Gilmore & D. Howell (San Fransicso: ASP), 157
Davis, M., Feigelson, E., & Latham, D. 1980, AJ, 85, 131
Djorgovski, S., & Meylan, G. 1994, AJ, 108, 1292
Elson, R. A. W., Tanvir, N., Gilmore, G., Johnson, R., & Beaulieu, S. 1999, in IAU Symp. 190, New Views of the Magellanic Clouds, ed. Y.-H. Chu, N. Suntzeff, J. Hesser, & D. Bohlender (San Francisco: ASP), in press
Feltzing, S., & Gilmore, G. 1999, preprint
Gilmore, G., & Howell, D., ed. 1998, ASP Conf. Ser. 142, The Stellar Initial Mass Function (San Francisco: ASP)
Gilmore, G., & Unavane, M. 1998, MNRAS, 301, 813
Grillmair, C., et al. 1998, AJ, 115, 144
Hargreaves, J., Gilmore, G., & Annan, C. 1996, MNRAS, 279, 108
Hargreaves, J., Gilmore, G., Irwin, M. J., & Carter, D. 1994, MNRAS, 271, 693
Harris, W. E. 1996, AJ, 112, 1487
Hernandez, X., Gilmore, G., & Valls-Gabaud, D. 1999, MNRAS, in press
Holtzman, J., Burrows, J. B., Casertano, S., Hester, J. J., Trauger, J. T., Watson, A. M., & Worthey, G. 1995a, PASP, 107, 1065
Holtzman, J., et al. 1995b, PASP, 107, 156
Kroupa, P., Tout, C., & Gilmore, G. 1991, MNRAS, 251, 293
Mateo, M. 1998, ARA&A, 36, 435
Merritt, D., Meylan, G., & Mayor, M. 1997, AJ, 1074
Olszewski, E. W., & Aaronson, M. 1985, AJ, 90, 2221
Olszewski, E. W., Aaronson, M., & Hill, J. M. 1995, AJ, 110, 2120
Olszewski, E. W., Pryor, C., & Armandroff, T. 1996, AJ, 111, 750
Piatek, P., & Pryor, C. 1995, AJ, 109, 1071
Piotto, G., Cool, A., & King, I. R. 1997, AJ, 113, 1345
Shetrone, M., Bolte, M., & Stetson, P. 1998, AJ, 115, 1888